

SEISMIC FRAGILITY OF APR1400 MAIN STEAM PIPING SYSTEM

E. Salimi Firoozabad ¹, B.G. Jeon ², D.G. Hahm ³, N.S. Kim ¹

¹ Civil And Environmental Engineering, Pusan National University: Geumjeong-gu, Busan, Korea, 609735,
e.salimi@pusan.ac.kr, nskim@pusan.ac.kr

² Seismic Simulation Test Center, Pusan National University: Mulgeum, Yangsan, Korea, 626870, bkjeon79@pusan.ac.kr

³ Integrated Safety Assessment Division, Korea Atomic Energy Research Institute: Yuseong, Daejeon, Korea, 305600,
dhahm@kaeri.re.kr

Fragility analysis is a proven method for the estimation of the seismic performance of structures and related equipment against any possible earthquake. In this study the advanced power reactor of South Korea (APR1400) main steam piping system was simplified by making it symmetric in order to reduce computation time. The selected system was then taken for the fragility analysis considering a new failure criterion for the steel elbows. The seismic analysis of the piping system indicated that one of the elbow sections is the most critical point of the piping system. The previously performed monotonic and cyclic loading experiments on the different size of pipe components revealed the reliability of the corresponding finite element numerical analysis. Fragility curves are derived for elbow section as a function of the peak ground acceleration (PGA) of records and the defined maximum relative displacement (MRD). The failure point of the elbow is estimated through the damage calculation using Banon damage index and twice elastic slope (TES). The corresponding fragility curves are derived and the conservatism of the code provision definition of the failure point is pointed out.

I. INTRODUCTION

NPP seismic risk assessment has been the subject of extensive researches. Kennedy and Ravindra ¹ clarified the fragility parameters, equations and procedure, and key roles, based on probabilistic risk assessment of other NPPs. The study was providing the values for uncertainty and randomness of structural capacity and response for the NPP structure and its mechanical and electrical components. Another effort in this regard found that seismic isolation reduces NPP building, floor, and equipment responses ² (Eidinger and Kelly, 1985). The study investigates the technical and non-technical effects of seismic isolation to the NPPs. They provided valuable data on seismic isolation use around the world. In addition, the study by Huang et al. ³ shows that base isolation reduces the probability of unacceptable performance of NPP building and secondary systems by approximately four orders of magnitude.

The numerical computation of fragility of the NPP building and components based on nonlinear three-dimensional (3-D) finite element methods (FEM) (Ref. 4), the response surface (De Grandis et al., ⁵, Perotti et al., ⁶), and statistical simulation-based fragility assessments (Zentner, ⁷) have been also proposed. Chen and Soong ⁸ provided a comprehensive review on seismic responses of secondary structures connected to primary structures. Mizuno et al., ⁹ assessed the failure mode of base isolated NPP main steam piping system due to the low cycle ratcheting failure.

The seismic behavior of the piping systems under multiple supports have been investigated using different approaches by Leimbach and Sterkel ¹⁰, Xu et al., ¹¹, Kai et al. ¹². The seismic response of APR1400 piping system and the effect of base isolation on the piping response were also studied by Kim et al. ¹³, Surh et al. ¹⁴.

In this paper the seismic fragility of a simplified APR 1400 main steam piping system was carried out. The selected input motions were scaled according to the conditional mean spectrum (CMS) method and applied to the structures. The time history analysis of the base isolated NPP building was performed and the support responses were extracted to apply on the piping system. The seismic analysis of the piping system was performed by applying selected records and support excitations. The critical point of the piping system was identified and its corresponding fragility curves were derived for the most suitable seismic intensity parameters. The failure point of the elbows was defined as their damage capacity by Banon damage index. The paper also addresses the conservatism of the code provisions definition of the failure point of the piping system.

II. THE APR1400 STRUCTURE AND MAIN STEAM PIPING SYSTEM DESCRIPTION

The beam-stick element model of the base isolated APR1400 was taken as NPP structure and shown in Fig. 1. The model consists of reactor containment building (RCB) auxiliary building (AB) and moat structure. The beam stick model details can be found in Surh et al. ¹⁴ and Han et al. ¹⁵. The main steam piping system of the APR1400 (Fig. 1b) was taken to perform a seismic fragility analysis. The piping sizes and wall thickness are also given in Fig. 1b. It must be noted that the piping system taken in this study is not the complete system and also its geometry was slightly changed and simplified to be symmetric in order to decrease the computational time. Therefore the piping system taken for the analysis is half the simplified system by setting the symmetric boundary condition.

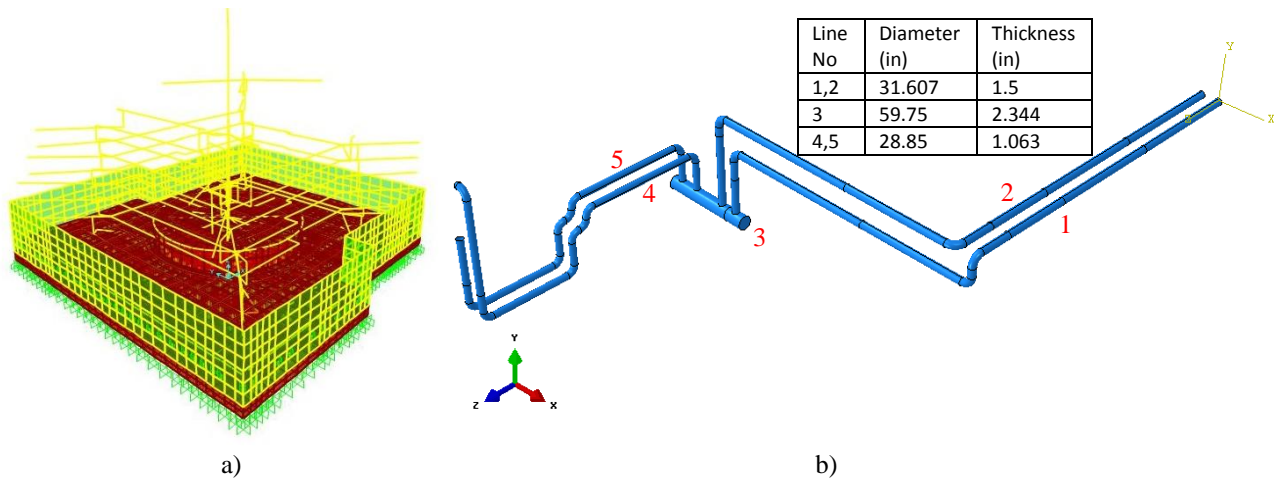


Fig. 1. (a) The NPP structure; (b) piping system.

III. NUMERICAL SIMULATION

I.A. Numerical model

A quadrilateral standard shell finite element (S4R) was used in the analysis that performed using ABAQUS 6.12. The piping system was attached in 34 locations with various restrictions on different elevations to the Auxiliary building (AB) and turbine pedestal. The boundary conditions and restricted locations are given in Fig. 2a and TABLE I. The material properties such as Young's modulus, Poisson ratio and density was taken as follows respectively, 30000 ksi, 0.28, 0.000786 lb/in³. The plastic properties was taken as kinematic hardening (shown in Fig. 2b). The geometric nonlinearity effect for the cyclic loading was also considered in order to capture the stiffness and strength degradation. Fig. 2c shows the meshed piping system.

TABLE I. Boundary Conditions of the Piping System

Support ID	Restricted directions	Restricted location
R1,2	X,Y,Z	AB 137.5 ft
R3,4,5,6	X,Y	AB 137.5 ft
R7,8,9,10	Y	AB 137.5 ft
R11,12	X,Z	AB 120 ft
T1	Y	AB 100 ft
P1,2	X,Y,Z	TP, ground level
P3,4	X	TP, ground level

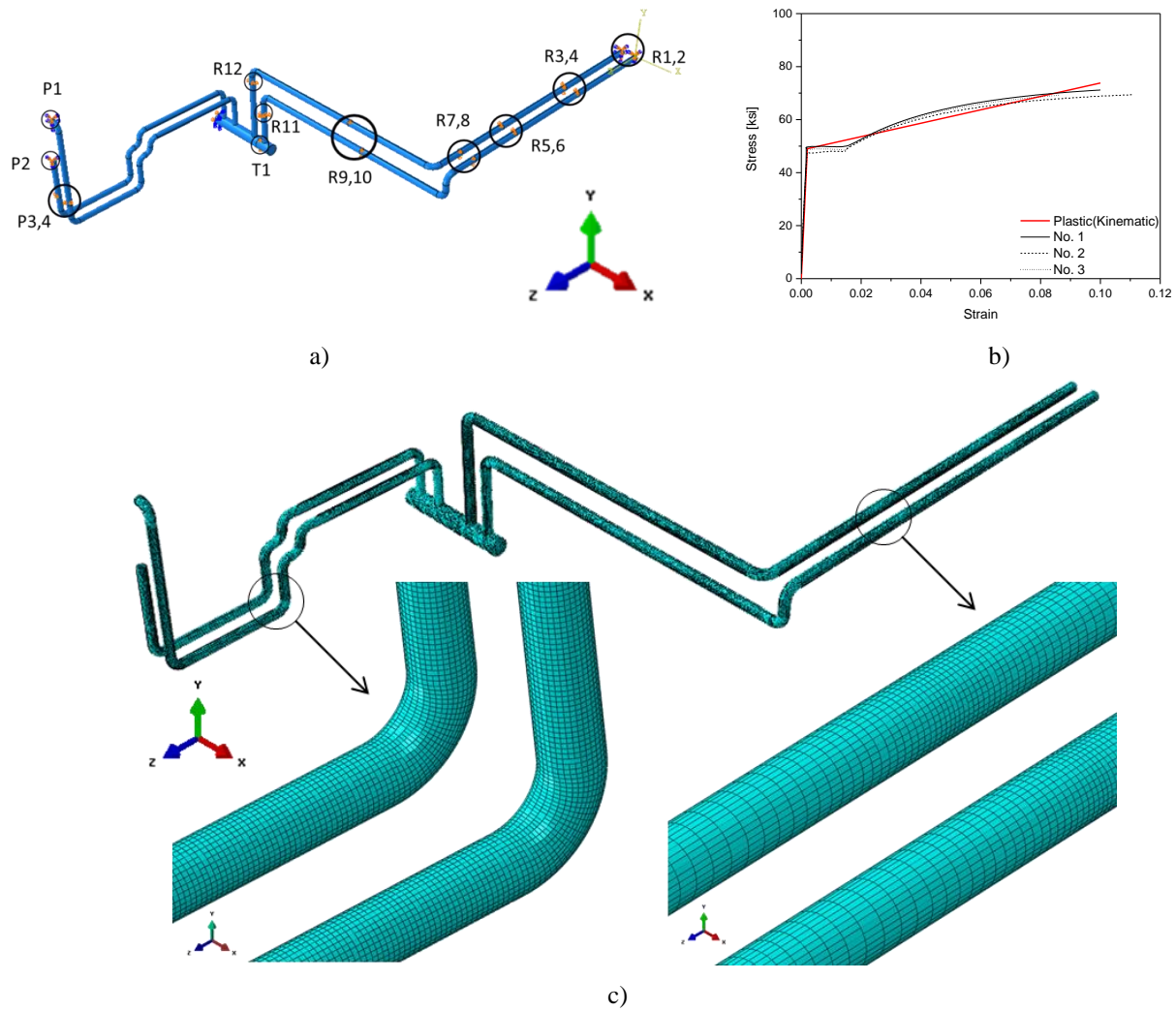


Fig. 2. (a) Support locations; (b) Plastic behavior of the materials; (c) the meshed piping system.

III.B. Validation of Numerical Analysis

A series of monotonic and cyclic loading experiments were previously performed on 3 and 12 inches elbow specimens. The simulation results of the structure performed in ABAQUS 6.12 were in good agreement with the experimental data. The comparative force-displacement curves indicate the reliability of the numerical simulations. The information on experimental setup, procedure, specimens and other detailed information can be found in Salimi Firoozabad et al.,^{16,17}

III.C. Seismic Record Selection and Scaling

In order to select and scale suitable number of seismic records, we have taken a hypothetical NPP location as in the western United States with longitude and latitude of 120.854° West and 35.207° North, located on a rock site (NEHRP class B site). The magnitude-distance (M, R) corresponding to this location is estimated as: (6.75, 6.7 km). Hence, a total of 20 records were selected within the magnitude range of 6.5 to 7, and a distance range between 0 and 32.7 km. The style of faulting and site classification was relaxed to overcome the issue of the number of sufficient records. The number of records seems rather suitable (more than 20 (Ref. 18)) in order to evaluate an accurate fragility function based on any ground motion intensities. The selected records and their characteristics are given in TABLE II.

The records were then scaled based on CMS scaling methodology¹⁹ in the period ($T = 2.1 s$) range of interest from $0.2T = 0.42 s$ to $2T = 4.2 s$. The details on record selection, calculation of CMS and scaling procedure can be found in Salimi Firoozabad et al.¹⁶

TABLE II. Selected record characteristics

Record ID	Record Name, location and Date	M (R)	D (km)	Vs30(m/s)	Fault Type
NGA0286	Irpinia, Italy-01 1980-11-23 19:34	6.9	17.51	1000	N
NGA3548	Loma Prieta 1989-10-18 00:05	6.93	3.22	1070.3	R
NGA0126	Gazli, USSR 1976-05-17	6.8	3.92	659.6	SS
NGA1111	Kobe, Japan 1995-01-16 20:46	6.9	7.08	609	SS
NGA0828	Cape Mendocino 1992-04-25 18:06	7.01	0	712.8	R
NGA0825	Cape Mendocino 1992-04-25 18:06	7.01	0	513.7	R
NGA0830	Cape Mendocino 1992-04-25 18:06	7.01	26.52	513.7	R
NGA0587	New Zealand-02 1987-03-02 01:42	6.6	16.09	424.8	N
NGA0957	Northridge-01 1994-01-17 12:31	6.69	15.87	821.7	R
NGA0989	Northridge-01 1994-01-17 12:31	6.69	9.87	740.1	R
NGA1011	Northridge-01 1994-01-17 12:31	6.69	15.11	1222.5	R
NGA1021	Northridge-01 1994-01-17 12:31	6.69	31.27	821.7	R
NGA1020	Northridge-01 1994-01-17 12:31	6.69	20.77	602.1	R
NGA1091	Northridge-01 1994-01-17 12:31	6.69	23.1	996.4	R
NGA0072	San Fernando 1971-02-09 14:00	6.61	19.45	821.7	R
NGA0071	San Fernando 1971-02-09 14:00	6.61	13.99	602.1	R
NGA0080	San Fernando 1971-02-09 14:00	6.61	21.5	969.1	R
NGA0495	Nahanni, Canada 1985-12-23	6.76	2.48	659.6	R
NGA0496	Nahanni, Canada 1985-12-23	6.76	0	659.6	R
NGA0497	Nahanni, Canada 1985-12-23	6.76	4.93	659.6	R

IV. SEISMIC ANALYSIS OF NPP STRUCTURE AND IDENTIFICATION OF THE SYSTEM CRITICAL POINT

The 20 selected and scaled records were applied (in SAP 2000) to the seismically-isolated primary structure (beam stick model) in Z direction. The displacement response of the connection points (the points at which the building structure and piping system are coupled) were extracted to be applied as the boundary condition in the analysis of the piping system. The input motions were applied on the support P1, 2 and P3, 4 where the piping system was attached to the turbine pedestal (taken as the ground level) and the other connection points in the piping system were shown in Fig. 2a. The displacement responses were extracted at the same elevation that the piping system was attached to the building structure. However, as the building structure is seismically isolated, the displacement responses were quite the same in all elevations.

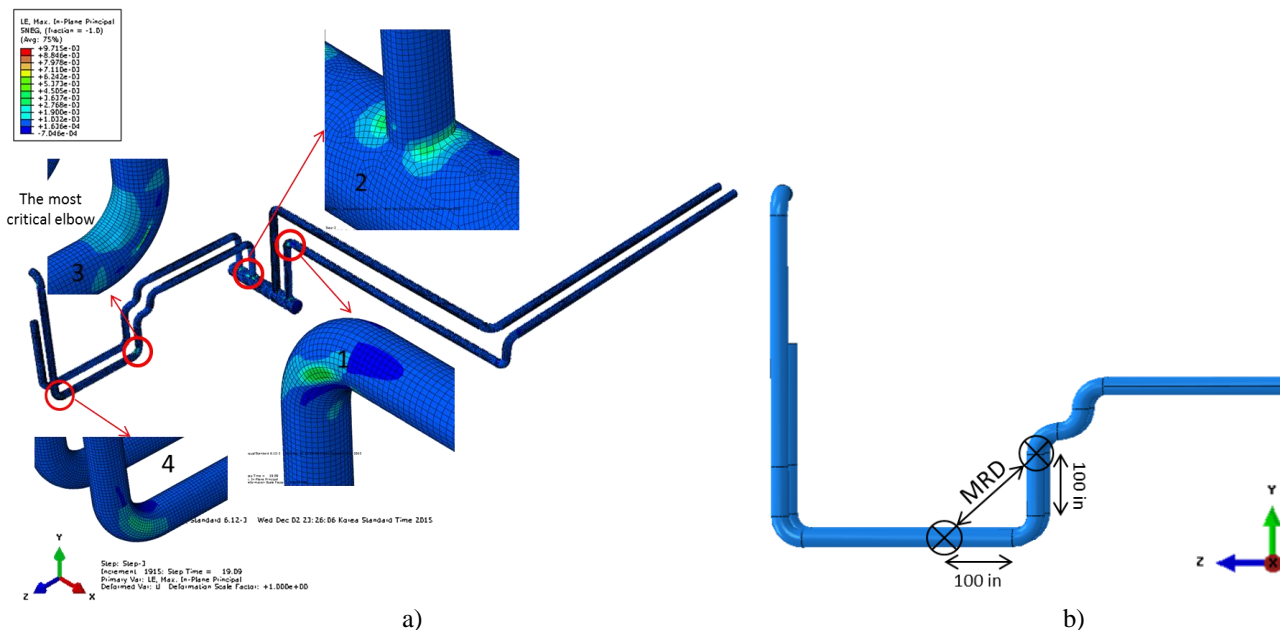


Fig. 3. (a)The max. in-plane strain contour and the critical points; (b) The location of displacement response for MRD

The analysis procedure of the piping system is divided into two steps; first a static analysis of the system is performed to consider the internal pressure (1200 psi which was a design pressure criterion for the APR1400). Second a dynamic implicit analysis of the system is performed to account for both the internal pressure and the seismic analysis. The displacement response of the connection points (the points at which the building structure and piping system are coupled) were extracted and applied as the boundary condition in the analysis of the piping system. The analysis was performed only in Z direction, the same procedure may be applied in X direction too. Hence, the fragility analysis would be performed in Z direction. Fig. 3 shows the maximum in-plane strain contour and the critical points of the piping system subjected to the motion in the Z direction. The simulation was also indicated that the most critical section was an elbow shown as 3 in Fig 3a.

Total number of records is 20, which were applied in Z directions for a total of 20 simulations. The maximum in-plane strain of the elbow (opening and closing modes) was considered as the seismic response parameter for the evaluation of fragility curves. The maximum relative displacements (MRDs) which are defined as the displacement response differences between both ends (shown in Fig. 3b) of the most critical elbow (elbow number 3 in Fig. 3a) were calculated to account for fragility estimation. The results are taken as the response of the system in each simulation case (presented in TABLE III for all records in the Z direction). It must be noted that the seismic response of piping system is given for both the closing and opening modes separately, as the structural behavior of the elbow is different in tension and compression.

TABLE III. Response of Piping System Due to Each Applied Record

No.	Record ID	Maximum relative displacement (MRD) (in)		Maximum in-plane strain	
		Closing	Opening	Closing	Opening
1	NGA0286	1.0061	1.3403	0.001654	0.002764
2	NGA3548	1.0575	1.0432	0.001802	0.002084
3	NGA0126	1.2998	1.6453	0.002196	0.003465
4	NGA1111	1.8082	1.8913	0.003	0.0058
5	NGA0828	0.8785	0.9458	0.00159	0.001867
6	NGA0825	1.5993	1.6744	0.002632	0.004252
7	NGA0830	3.5390	2.8575	0.019341	0.017793
8	NGA0587	1.3044	1.2666	0.002168	0.002466
9	NGA0957	1.0865	1.5152	0.001756	0.003357
10	NGA0989	1.2142	1.1970	0.00187	0.002364
11	NGA1011	1.9615	1.9070	0.003943	0.00602
12	NGA1021	2.5440	2.5717	0.009399	0.010131
13	NGA1020	2.4391	1.9222	0.006583	0.008154
14	NGA1091	1.5676	1.5148	0.002694	0.00367
15	NGA0072	1.9025	2.2626	0.00995	0.009684
16	NGA0071	2.6062	2.9679	0.018699	0.014579
17	NGA0080	1.8466	2.1926	0.006078	0.009474
18	NGA0495	1.9152	1.9208	0.003356	0.006723
19	NGA0496	1.6068	1.6494	0.002637	0.004096
20	NGA0497	2	2.2610	0.007343	0.009226

V. SEISMIC FRAGILITY ANALYSIS

The seismic fragility analysis of the piping system is represented as the fragility curves of the elbow (the most critical) section for both the opening and closing mode. The seismic response of the piping system has already been obtained and the responses were shown as the maximum strain of the elbow induced by any individual input motions. The next steps would be the estimation of the failure criteria of the elbow component, selection of seismic intensity parameters, and determination of the method of fragility estimation.

V.A. Failure criteria of the piping system

The twice elastic slope method (TES) for the force-strain or displacement curve is adopted by the American Society of Mechanical Engineers (ASME) (Ref. 20) for the plastic limit load material criterion. In this study, the ASME criterion (TES) was used to estimate the collapse strain point of the elbow section of the piping system. Hence, the force-strain curve of the elbow in both the opening and closing modes were evaluated, and the maximum strain was calculated using the TES method.

Fig. 4 shows the estimated force-strain curves based on updated numerical simulation, and the calculated maximum strain for each case and the plastic limit strain is estimated as 0.0064 and 0.0088 for the elbow closing and opening mode, respectively.

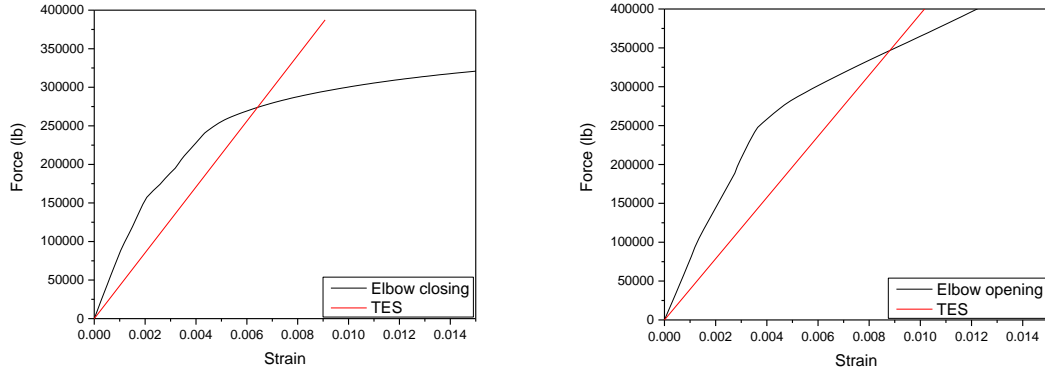


Fig. 4. The plastic limit strain based on TES method

The failure point of the elbow component was represented in the Salimi Firoozabad et al.,¹⁷ as the damage capacity of the structure. Based on our experimental results, presented and explained¹⁷, it became clear that the failure of a steel pipe elbow can be expressed by Banon²¹ damage indices. It was observed that the failure point of the elbow can be calculated using the Banon damage index quite well. Hence, in the present study, the failure point of the elbow component is taken as the damage capacity of elbow calculated based on the experimental results by using Banon damage indices under repeated cyclic loading.

$$D = \sqrt{\left(\max(D_i/D_y - 1)\right)^2 + \left(\sum_{i=1}^N c \cdot (2E_i/F_y \cdot D_y)^d\right)^2} \quad (1)$$

where D_y, F_y are the yield displacement and force; D_i, E_i are the displacement and dissipated energy in the i -th cycle; and N is the number of cycles. The procedure was examined under constant and non-constant loading histories, and the constant c and d was optimized as 3.3 and 0.21. It must be noted that, the experiment were performed on the 3 inches elbow specimens. It was also examined for an 8 inches component based on the experimental results performed at Delft University of Technology, and reported by Varelis et al.²² It was observed that the average estimated damage of the 3 inches elbow component (13.79) was almost the same as that of the 8 in elbow (13.37). Hence the failure criterion is taken as the damage corresponding to the average failure Banon damage of 3 and 8 inches specimens which is equal to 13.63 $((13.79+13.37)/2)$.

In order to use the damage indices to estimate the structural capacity, it is necessary to calculate the structural response by using the damage indices. Hence, the displacement responses of both end (100 inches from the elbow) of the elbow were extracted from the simulations performed on the piping system for each input motions. The displacement differences of both ends of the elbow were calculated for all 20 input motions in order to apply on the elbow model. The elbow was modeled separately, using the same geometry and properties as the piping system with 100 inches elbow length for each end (Fig. 5 shows the elbow geometry and model). The same elbow was used to estimate the force-strain curves to obtain TES. The numerical simulations on elbow were performed statically; the force-displacement curves were drawn and used to calculate the damage of the structure.

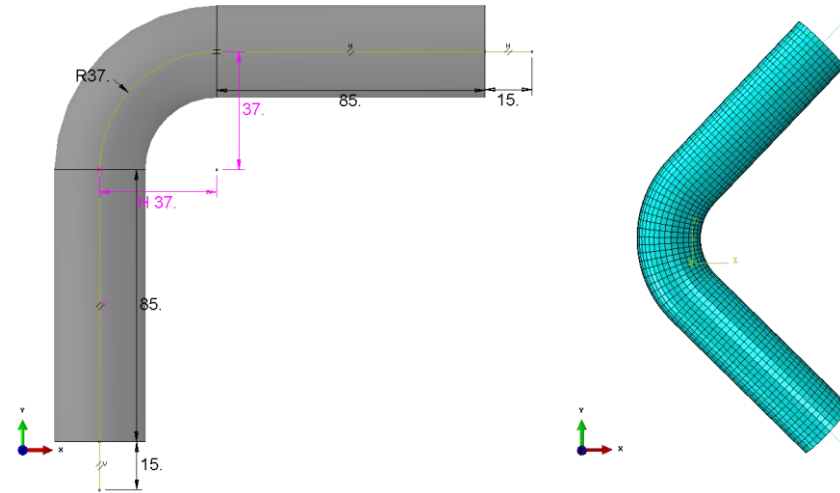


Fig. 5. The critical elbow model: geometric description; Meshed elbow

V.B. Seismic intensity parameter selection

In the application of fragility analysis, the maximum in-plane strain of critical elbow section is taken as the seismic response parameter. The conditional probability of failure can be expressed as a function of different seismic intensity parameters which must be proved to sufficiently describe the ground motion response. The regression analysis was performed on PGA and Sa (at natural period of the structure) seismic intensities and the MRD of the piping system in order to determine the correlation of those intensities with the seismic response of the system.

The seismic intensity-response relationship is expressed as correlation coefficient (R^2) of the predicted equation. The seismic intensities including the PGA and Sa at the natural period of the structure ($T = 2.1s$) were considered to perform regression analysis. The correlation of coefficients for the first-order predicted equation between each considered seismic intensity and seismic response (maximum in-plane strain) for the elbow were given in TABLE IV.

TABLE IV. Estimated Correlation Coefficient for Each Seismic Intensity

Seismic intensity	Correlation coefficient (R^2)	
	Closing mode	Opening mode
PGA	0.7458	0.7528
Sa ($T = 2.1s$)	0.0591	0.0823
MRD	0.7612	0.904

Based on the regression analysis results shown in Table 4, the maximum in-plane strain (the seismic response) does not correlate (R^2 value less than 0.1) with the spectral acceleration (Sa ($T = 2.1s$)) of the records. However, the peak ground acceleration (PGA) correlates quite well (0.75) with the seismic response. Thus, we suggest that, the fragility curves can be estimated for the MRD and PGA which were correlated quite well (R^2 more than 0.75) with seismic responses in order to perform the fragility analysis.

V.B. Fragility analysis

The probability of failure $P_f(e)$ concerning a certain seismic response parameter for a given seismic intensity e is the probability of the ratio of its seismic capacity C to the seismic response parameter $R(e)$. Under the assumption that R and C are log-normally distributed, the following expression is given for fragility²³:

$$P_f(e) = \phi\left(\frac{\ln R_m(e) - \ln C_m}{\sqrt{\beta_r^2 + \beta_c^2}}\right) \quad (2)$$

where ϕ is the cumulative function of the standard normal distribution, $R_m(e)$ and C_m are the median values of the seismic response $R(e)$ and capacity C , respectively; and β_r, β_c are the log-normal standard deviations of C and $R(e)$.

The fragility curve of the piping system was estimated, and is shown in Fig. 8 as the fragility of the elbow as a function of the MRD and PGA using the estimated failure criteria based on both the TES and Banon damage index. The fragility of the elbow section was obtained for the closing and opening modes in the Z directions. In order to compare the probability of failure of the elbow, the closing and opening mode curves are shown in the same figure.

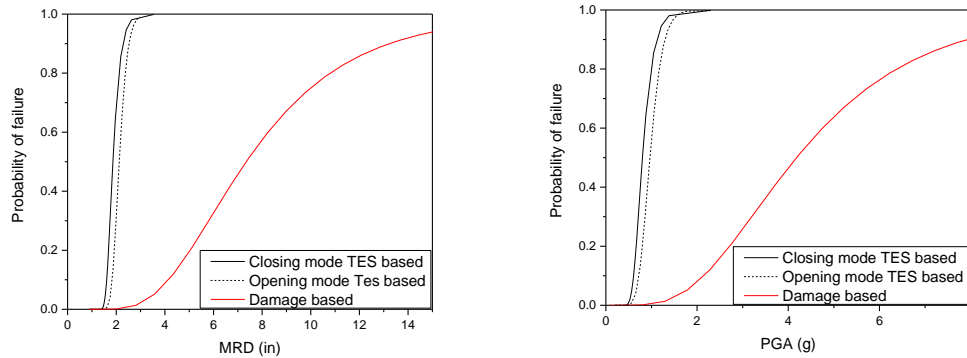


Fig. 6. Fragility curves of the elbow based on Banon damage index failure criteria.

In order to evaluate the probability of failure of the elbow section, we have been already noted that the fragility evaluation must be carried out for both the closing and opening modes. Fig. 6 shows the difference between closing and opening mode for the MRD and PGA case of fragility estimation. It was seen that the more critical mode is the closing mode in both functions MRD and PGA.

The failure criterion of the elbow component has been already carried out through its damage capacity by using Banon damage index. Hence, the fragility curves of the component were also estimated by using this failure point and it is shown in Fig. 6. It was observed that the probability of failure decreased when we changed the capacity estimation from TES to its damage capacity. The high confidence of low probability of failure (5% HCLPF) in the case of MRD increased from 1.55" (closing) and 2.12" (opening) in TES based to 3.58" in damage based failure estimation. In the case of PGA also, almost the same difference can be seen. The 5% HCLPF is given for all cases in TABLE V. That difference indicates the conservatism of setting the failure point of the elbow as twice its elastic slope.

TABLE V. High Confidence of Low Probability of Failure (HCLPF) in Each Case of Fragility Estimation

Seismic intensity	5% HCLPF		
	TES based		Damage based
	Closing mode	Opening mode	
PGA (g)	0.57	0.68	1.71
MRD (in)	1.55	2.12	3.58

VI. CONCLUSIONS

The maximum relative displacement between the described points and PGA of records is a suitable function for fragility analysis. Regarding the difference between the capacity of the elbow in opening and closing mode, it is well indicated that the fragility of the section must be evaluated for both modes.

The failure criteria of the elbow components were represented as the damage capacity by using damage indices available in the literature. It was observed that the damages calculated through the Banon damage index, for all the considered loading histories are very similar.

The procedure to use the damage capacity as a failure criterion for the elbow was experimentally examined on 3 and 8 in. specimens. It was observed that the calculated Banon damage results was almost constant for all loading histories (constant and non-constant) although, the properties, geometry and loading condition was very different in two performed experiments.

The comparison of fragility curves obtained based on both methods for failure estimation indicated that TES method is a conservative way to set the failure point. It was shown that the HCLPF is approximately twice in damage based compared to the TES based failure estimation.

ACKNOWLEDGMENTS

This work was supported by the energy efficiency and resources of Korea Institute of Energy Technology Evaluation and Planning (KIETEP) grant, funded by the Ministry of Knowledge Economy (MKE) of the Korean government (no. 2014151010170C).

REFERENCES

1. R. P. KENNEDY and M. K. RAVINDRA, "Seismic Fragilities for Nuclear Power Plant Risk Studies," *Nuclear Engineering and Design*, 79, 47-68 (1984).
2. J. M. Eidinger and J. M. Kelly, "Seismic isolation for nuclear power plants: technical and non-technical aspects in decision making," *Nuclear Engineering and Design*, 84(3):383-409 (1985).
3. Y. N. Huang, A. S. Whittaker, and N. Luco, "Seismic performance assessment of base-isolated safety-related nuclear structures," *Earthquake Engineering & Structural Dynamics*, 39.13: 1421-1442 (2010).
4. N. Nakamura, S. Akita, T. Suzuki, M. Koba, S. Nakamura, and T. Nakano, "Study of ultimate seismic response and fragility evaluation of nuclear power building using nonlinear three-dimensional finite element model," *Nuclear Engineering and Design*, 240(1), 166-180 (2010).
5. S. De Grandis, M. Domaneschi, and F. Perotti, "A numerical procedure for computing the fragility of NPP components under random seismic excitation," *Nuclear Engineering and Design*, 239.11: 2491-2499 (2009).
6. F. Perotti, M. Domaneschi, and S. De Grandis, "The numerical computation of seismic fragility of base-isolated Nuclear Power Plants buildings," *Nuclear Engineering and Design*, 262: 189-200 (2013).
7. I. Zentner, "Numerical computation of fragility curves for NPP equipment," *Nuclear Engineering and Design*, 240.6: 1614-1621 (2010).
8. Y. Chen, and T. T. Soong, "Seismic response of secondary systems," *Engineering Structures*, 10(4), pp.218-228 (1988).
9. K. Mizuno, H. Shimizu, M. Jimbo, N. Oritani, and S. Onishi, "Development of an Evaluation Method for Seismic Isolation Systems of Nuclear Power Facilities: Part 5 Fatigue Test of the Crossover Piping," *ASME 2014 Pressure Vessels and Piping Conference* (pp. V008T08A039-V008T08A039) American Society of Mechanical Engineers, (2014).
10. J. Xu, G. DeGrassi, and N. Chokshi, "A NRC-BNL benchmark evaluation of seismic analysis methods for non-classically damped coupled systems," *Nuclear engineering and design*, 228.1: 345-366 (2004).
11. K. R. Leimbach, and H. P. Sterkel, "Comparison of multiple support excitation solution techniques for piping systems," *Nuclear Engineering and Design*, 57(2), 295-307 (1980).
12. S. Kai, A. Otani, and N. Kaneko, "Analytical Study on Seismic Response of Piping under Multiple Support Excitations," In *ASME 2012 Pressure Vessels and Piping Conference* (pp. 37-43). American Society of Mechanical Engineers (2012).
13. D. S. Kim, J. H. Lee, and I. Y. Kim, "A Parametric Study of Independent Support Motion Method for the Steam Supply Piping Connected to the HP Turbine of APR 1400," In *ASME 2013 Pressure Vessels and Piping Conference* (pp. V008T08A023-V008T08A023), American Society of Mechanical Engineers (2013, July).
14. H. B. Surh, T. Y. Ryu, J. S. Park, E. W. Ahn, C. S. Choi, J. C. Koo, and M. K. Kim, "Seismic response analysis of a piping system subjected to multiple support excitations in a base isolated NPP building," *Nuclear Engineering and Design*, 292, 283-295 (2015).
15. S.R. Han, M.J. Nam, C.G. Seo, and S.H. Lee, "Soil-structure interaction analysis for base-isolated nuclear power plants using an iterative approach," *J. Earthquake Eng. Soc. Korea* 19, 21-28 (2015).
16. E. S. Firoozabad, B. G. Jeon, H. S. Choi, and N. S. Kim, "Seismic fragility analysis of seismically isolated nuclear power plants piping system," *Nuclear Engineering and Design*, 284, 264-279 (2015).
17. E. S. Firoozabad, B. G. Jeon, H. S. Choi, and N. S. Kim, "Failure criterion for steel pipe elbows under cyclic loading," *Engineering Failure Analysis*, 66, 515-525 (2016).
18. G. P. Cimellaro, A. M. Reinhorn, A. D'Ambrisi, and M. De Stefano, "Fragility analysis and seismic record selection," *Journal of Structural Engineering*, 137(3), 379-390 (2009).
19. J. W. Baker, "Conditional Mean Spectrum: Tool for ground motion selection," *Journal of Structural Engineering*, 137(3), 322-331 (2011).
20. American Society of Mechanical Engineers (ASME), Boiler and Pressure Vessel Code (2007).
21. H. Banon, H. M. Irvine, and J. M. Biggs, "Seismic damage in reinforced concrete frames," *Journal of the Structural Division*, 107(9), 1713-1729 (1981).
22. G. E. Varelis, S. A. Karamanos, and A. M. Gresnigt, "Pipe Elbows Under Strong Cyclic Loading," *Journal of Pressure Vessel Technology*, 135(1), 011207 (2013).
23. S. L. Dimova, and K. Hirata, "Simplified seismic fragility analysis of structures with two types of friction devices," *Earthquake Engng. Struct. Dyn.*, 29: 1153-1175 (2000).